

Centaurus A as the Source of ultra-high energy cosmic rays?

Claudia Isola^a, Martin Lemoine^b, Günter Sigl^b

^a *Centre de Physique Théorique,*

Ecole Polytechnique, 91128 Palaiseau Cedex, France

^b *Institut d'Astrophysique de Paris, C.N.R.S., 98 bis boulevard Arago, F-75014 Paris, France*

(April 13, 2001)

We present numerical simulations for energy spectra and angular distributions of nucleons above 10^{19} eV injected by the radio-galaxy Centaurus A at a distance 3.4 Mpc and propagating in extra-galactic magnetic fields in the sub-micro Gauss range. We show that field strengths $B \simeq 0.3\mu\text{G}$, as proposed by Farrar & Piran, cannot provide sufficient angular deflection to explain the observational data. A magnetic field of intensity $B \simeq 1\mu\text{G}$ could reproduce the observed large-scale isotropy and could marginally explain the observed energy spectrum. However, it would not readily account for the $E = 320 \pm 93$ EeV Fly's Eye event that was detected at an angle 136° away from Cen-A. Such a strong magnetic field also saturates observational upper limits from Faraday rotation observations and X-ray bremsstrahlung emission from the ambient gas (assuming equipartition of energy). This scenario may already be tested by improving magnetic field limits with existing instruments. We also show that high energy cosmic ray experiments now under construction will be able to detect the level of anisotropy predicted by this scenario. We conclude that for magnetic fields $B \simeq 0.1 - 0.5\mu\text{G}$, considered as more reasonable for the local Supercluster environment, in all likelihood at least a few sources within $\simeq 10$ Mpc from the Earth should contribute to the observed ultra high energy cosmic ray flux.

I. INTRODUCTION

In acceleration scenarios ultra high energy cosmic rays (UHECRs) with energies above 10^{18} eV are assumed to be protons accelerated in powerful astrophysical sources. During their propagation, for energies above $\gtrsim 50$ EeV ($1\text{EeV} = 10^{18}\text{eV}$) they lose energy by pion production and pair production (protons only) on the microwave background. For sources further away than a few dozen Mpc this would predict a break in the cosmic ray flux known as Greisen-Zatsepin-Kuzmin (GZK) cutoff [1], around 50 EeV. This break has not been observed by experiments such as Fly's Eye [2], Haverah Park [3], Yakutsk [4], Hires [5] and AGASA [6], which instead show an extension beyond the expected GZK cutoff and events above 100 EeV. This situation has in recent years triggered many theoretical explanations ranging from conventional acceleration to new physics as well as the construction of large new detectors [7].

In bottom-up scenarios of UHECR origin, in which protons are accelerated in powerful astrophysical objects such as hot spots of radio galaxies and active galactic nuclei [8], one would expect to see the source in the direction of arrival of UHECRs. The lack of observed counterparts to the highest energy events [9,10] implies the existence of large scale intervening magnetic fields with intensity $B \sim 0.1 - 1\mu\text{G}$ [10], which would provide sufficient angular deflection, or bursting sources and a magnetic field of intensity $B \gtrsim 10^{-11}$ G which would impart sufficient time delay to UHE protons to explain their lack of correlation in time of arrival with optical or high energy

photons [11]. It has been realized recently that magnetic fields as strong as $\simeq 1\mu\text{G}$ in sheets and filaments of large scale structure, such as our Local Supercluster, are compatible with existing upper limits on Faraday rotation [12–14].

Such strong magnetic fields would have profound consequences for the propagation of charged ultra-high energy cosmic rays [15–17]. In particular in the presence of a magnetic field of strength $B \simeq 0.1\mu\text{G}$, and for a source at distance $\simeq 10$ Mpc, UHECRs with energy $E \lesssim 100$ EeV would diffuse, while higher energy cosmic rays would propagate rectilinearly. The resulting modification of the energy spectrum would explain naturally the observed spectrum for a unique power-law injection of index $\simeq 2.2$. In Ref. [17], we further showed that a large number of such sources in the Local Supercluster, at distance scale $\simeq 10$ Mpc and an ambient magnetic field $B \simeq 0.1\mu\text{G}$ would explain the large scale isotropy of arrival directions observed by AGASA [6]. It would also explain the observed small-scale angular clustering (five doublets and one triplet within 2.5° out of 57 events above 40 EeV) by magnetic lensing effects through the large scale turbulent magnetic field.

At first sight this suggests the possibility of having only one object in the Sky as the source of all UHECRs with $E \gtrsim 5\text{EeV}$, including the highest energy events. Two versions of such single source scenarios have recently been put forward in the literature: one with an extreme version of a coherent Galactic magnetic wind structure in which all observed UHECRs supposedly can be traced back to M87 in the Virgo cluster [18], and a second

one with Centaurus A at 3.4 Mpc distance with an all-pervading magnetic field of intensity $B \simeq 0.3 \mu\text{G}$ [19]. In the present paper we examine critically the latter of these scenarios using detailed numerical simulations for the energy spectrum and the angular distribution of UHECRs propagating in magnetic fields of r.m.s. strength between 0.3 and $1 \mu\text{G}$.

II. NUMERICAL SIMULATIONS

Trajectories are calculated from the Lorentz equation in a given magnetic field and pion production is treated as stochastic energy loss while pair production is included into the equations of motion as a continuous energy loss term. This numerical tool has been used and discussed in earlier publications [16,17].

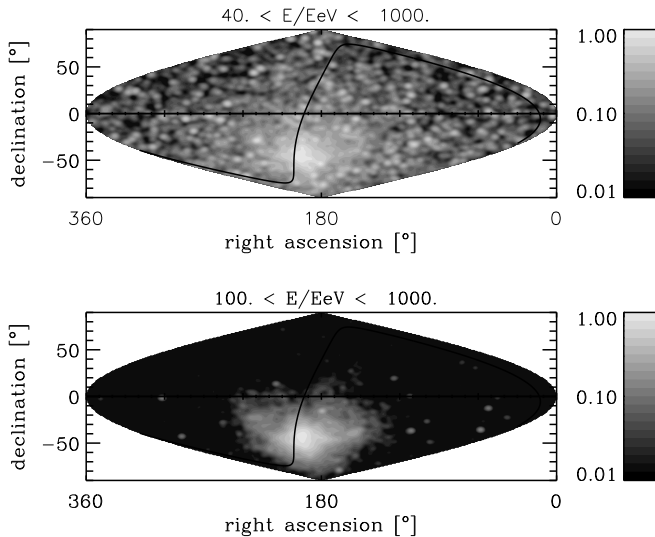


FIG. 1. The angular image in terrestrial coordinates, averaged over all 20 magnetic field realizations of 5000 trajectories each, for events above 40 EeV (upper panel) and above 100 EeV (lower panel), as seen by a detector covering all Earth, for the case suggested in Ref. [19] corresponding to $B = 0.3 \mu\text{G}$, and the source Cen-A located 3.4 Mpc away. The grey scale represents the integral flux per solid angle. The solid line marks the Supergalactic plane. The pixel size is 1° ; the image has been convolved to an angular resolution of 2.4° corresponding to AGASA.

We assume a homogeneous random turbulent magnetic field with power spectrum $\langle B(k)^2 \rangle \propto k^{n_B}$ for $2\pi/L < k < 2\pi/l_c$ and $\langle B^2(k) \rangle = 0$ otherwise. We use $n_B = -11/3$, corresponding to Kolmogorov turbulence, in which case L , the largest eddy size, characterizes the coherence length of the magnetic field; we use $L \simeq 1 \text{ Mpc}$, which corresponds to a few turn-arounds in a Hubble time. Physically one expects $l_c \ll L$, but numerical resolution limits us to $l_c \gtrsim 0.008L$. We generally use $l_c \simeq 0.03 \text{ Mpc}$, but we checked by increasing the resolution for several

runs that it has no effect on the results discussed in the following. The magnetic field modes are dialed on a grid in momentum space according to this spectrum with random phases and then Fourier transformed onto the corresponding grid in location space. The r.m.s. strength B is given by $B^2 = \int_0^\infty dk k^2 \langle B^2(k) \rangle$.

Typically, 5000 trajectories are computed for each magnetic field realization obtained in this way for 10-20 realizations in total. Each trajectory is followed for a maximal time of 10 Gyr and as long as the distance from the observer is smaller than double the source distance. We have also checked that the results do not significantly depend on these cut-offs. Furthermore, the distance limit is reasonable physically as it mimics a magnetic field concentrated in the large scale structure, with much smaller values in the voids, as generally expected.

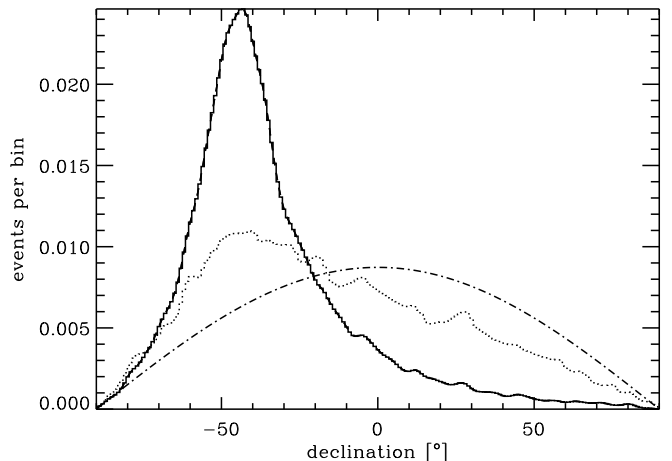


FIG. 2. The distribution of arrival declination on Earth, averaged over many realizations, for $E \geq 40 \text{ EeV}$ (dotted line) and $E \geq 100 \text{ EeV}$ (solid line), for the scenario corresponding to Figs. 1. The dash-dotted line represents an isotropic distribution. The pixel size is 1° and the image has again been convolved with an angular resolution of 2.4° .

In Fig. 1, we show the angular distribution of UHE events as seen on Earth in equatorial coordinates, for two ranges of energies $E \gtrsim 40 \text{ EeV}$, and $E \gtrsim 100 \text{ EeV}$, and for $B = 0.3 \mu\text{G}$, with Cen-A as the source. These images are averaged over different spatial realizations of the magnetic field. The distributions for specific realisations are more anisotropic than the average due to cosmic variance. The angular distribution predicted by this one source model is thus not consistent with the isotropic distribution deduced by experimental data [2,6]. This is even more clearly demonstrated by Fig. 2, which gives the distribution in declination of arrival coordinates of UHE events. The source Cen-A is located at $\text{RA} = 201.3^\circ$, $\delta = -43.0^\circ$ in equatorial coordinates, and corresponds to the peak of flux in Figs. 1,2.

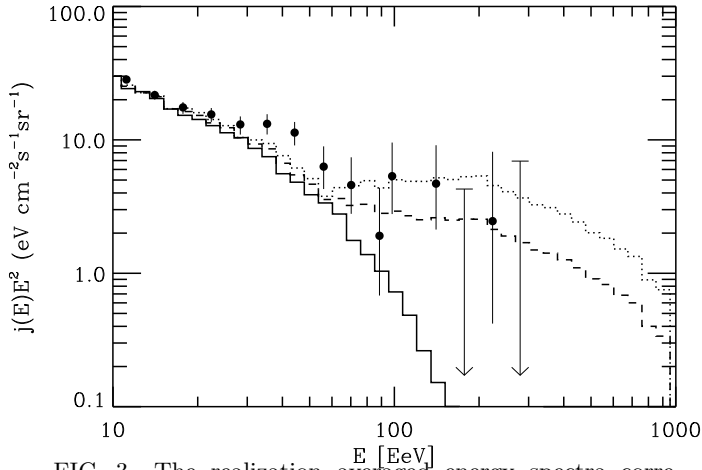


FIG. 3. The realization averaged energy spectra corresponding to Figs. 1,2. The solid line represents the spectrum that would have been detected by AGASA, and has been obtained from Eq. (1). The dashed line indicates the spectrum uniformly averaged over the whole sky. The dotted line is the spectrum predicted by an AGASA type experiment in the Southern hemisphere. The one sigma error bars indicate the AGASA data. The various spectra have been normalized to optimally fit the AGASA flux. Significant uncertainties due to cosmic variance and parameters such as the largest eddy size L only occur for energies between $\simeq 70$ EeV and a few hundred EeV where they are still smaller than a factor $\simeq 2.5$.

Cen-A does not lie in the field of view of experiments that have provided data so far such as the Fly's Eye and AGASA. This and the fact that the angular deflection of particles with $E \gtrsim 100$ EeV is relatively small has an important consequence for the energy spectrum predicted by this model: The Northern hemisphere experiments should never have detected the highest energy events, for which the angular deflection is too weak to bring the particle in the field of view. This is made clear in Fig. 3, where we compare the spectrum predicted for AGASA with the actually observed spectrum, assuming an injection spectrum $\propto E^{-2}$ up to 10^{21} eV. The prediction is obtained by folding the simulated distribution in energy E and arrival direction Ω , $D(E, \Omega)$, with the normalized AGASA exposure function $AGASA(\delta)$ (which to a good approximation only depends on declination δ):

$$j(E) \equiv \int d\Omega D(E, \delta) AGASA(\delta). \quad (1)$$

For reference, we also show in Fig. 3 the spectrum that would be observed by an idealized detector covering the whole sky uniformly, and by a mirror AGASA experiment located in the Southern hemisphere. The solid angle integrated spectrum $\int d\Omega D(E, \delta)$ observed by a uniform detector is still different from the injection spectrum ($\propto E^{-2}$) at low energies, while the two match at high energies. This results from an increased local residence time due to diffusion at low energies, and rectilinear propagation (hence unaffected energy spectrum) at high energies [16]. The pile-up around $E \simeq 40$ EeV due to pion

production of higher energy particles, also contributes to the change of slope at low energies.

The scenario just discussed, which is already ruled out by the energy spectrum and large-scale isotropy recorded by Northern hemisphere detectors, has been proposed by Farrar & Piran [19] on analytical grounds to explain all observational data. The discrepancy, as will be discussed in greater detail in Section 3, results from the fact that they argued that diffusion held up to the highest energies, whereas in fact the diffusion approximation breaks for $E \gtrsim 100$ EeV, implying much larger anisotropies at these energies. The impact of angular anisotropy on the energy spectrum for a source located in the blind area of Northern hemisphere detectors had also been overlooked in Ref. [19].

For the scenario with $B = 0.3 \mu\text{G}$ we have also established a rough estimate of the minimal number of sources necessary to explain existing observations in the following way: We overlaid distributions from single sources in random directions (for simplicity chosen to be at equal distances as Cen-A) and computed the average and fluctuations of the declination distributions of UHECR arrival directions. The minimal number of sources is determined by requiring that the distribution is consistent with isotropy within the fluctuations and turns out to be 5–10.

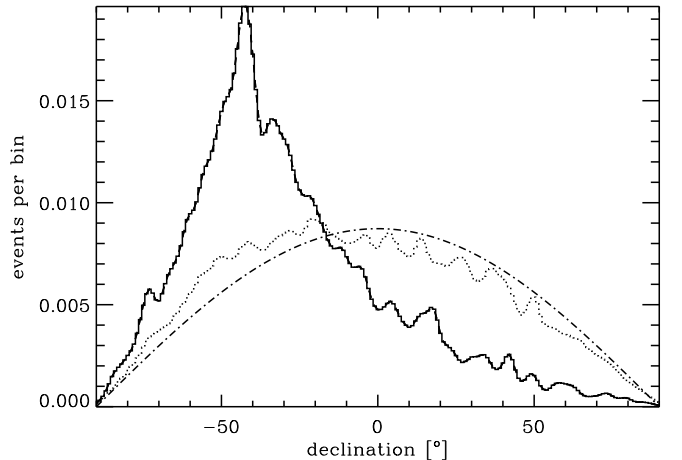


FIG. 4. The distribution of arrival declination on Earth, averaged over many realizations, for $E \geq 100$ EeV (dotted line) and $E \geq 300$ EeV (solid line). All other parameters are as in Fig. 2, expect $B = 1 \mu\text{G}$.

We now investigate whether stronger magnetic fields, by providing larger angular deflection, might provide a better match to the observational data. In particular, we focus on the case where $B = 1 \mu\text{G}$, and Cen-A is again the unique source of UHECRs. The resulting arrival distribution in declination is shown for several ranges of energies in Fig. 4, and the resulting energy spectra, calculated as before, is shown in Fig. 5. Increasing the magnetic field strength increases the maximal energy at which diffusion takes place, hence it decreases the

anisotropy at each energy up to that maximal energy, and thus reduces the differences between the spectra seen by different detectors (AGASA, uniform, and Southern hemisphere analogue of AGASA).

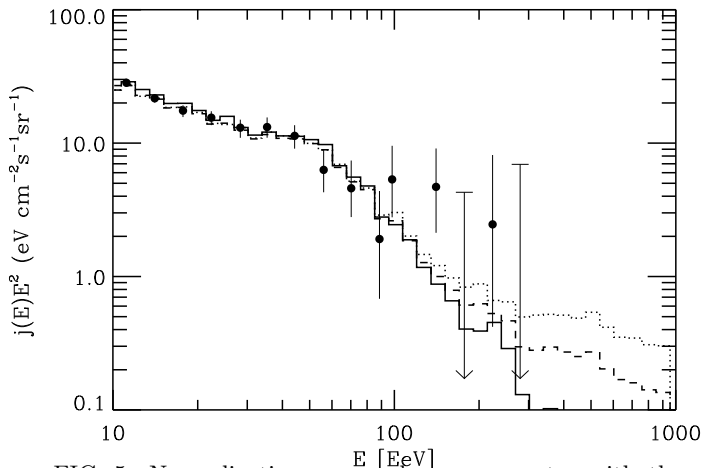


FIG. 5. Normalization averaged energy spectra with the same conventions as in Fig. 3, but for $B = 1 \mu\text{G}$, all other parameters being equal.

The large-scale anisotropy in this case is much smaller and could not have been detected by Northern hemisphere experiments such as the Fly’s Eye and AGASA. The predicted energy spectrum for AGASA does provide a very good fit to the observed spectrum, see Fig. 5, but the difference is not sufficient to rule out this scenario on this ground. However, we note that it is unlikely that the highest energy Fly’s Eye event would have been detected in this model. This event of energy $E = 320 \pm 93 \text{ EeV}$ makes an angle of 136° with the line of sight to Cen-A [10]. By folding the energy probability distribution for the Fly’s Eye event with the simulated distribution of deflection angles and energies one finds that 95% of events with a recorded energy corresponding to the Fly’s Eye event are deflected less than $\simeq 130^\circ$.

Thus the present observational evidence is not sufficient to rule out with a high degree of confidence the possibility that Cen-A is the source of all ultra-high energy cosmic rays, *if* the intervening magnetic field $B \gtrsim 1 \mu\text{G}$. Notably, one cannot rule out the possibility of having a magnetic configuration different from Kolmogorov turbulence, in which case the modification of the energy spectrum would be different than what is shown in the present simulations. For instance, it has been proposed that the magnetic field is not all pervading, but strongly enhanced in regions close to radio-galaxies that were active in the past [10,20], in which case the configuration seen by UHECRs would be a collection of scattering centers rather than Kolmogorov turbulence.

However, if future or ongoing experiments in the Northern hemisphere, e.g. the High Resolution Fly’s Eye [5] and AGASA [6] keep recording cosmic rays above $\simeq 200 \text{ EeV}$ with large deflection angles from the line

of sight to Cen-A, even the scenario with $B \simeq 1 \mu\text{G}$ would be unequivocally ruled out. Similarly, if no significant anisotropy is seen between these experiments and the Pierre Auger project [21] at the highest energies, the model would be discarded. As an example, we calculate from Eq. (1) the fractional difference $\delta I \equiv (I_N - I_S)/(I_N + I_S)$ of integral fluxes I_N and I_S that would be seen by detectors in the Northern and Southern hemispheres above a given energy (for simplicity, we use exposure functions for AGASA and an analogous one for the Southern hemisphere, as before). We find $\delta I \simeq -0.19$ for $E \gtrsim 100 \text{ EeV}$, and $\delta I \simeq -0.78$ for $E \gtrsim 300 \text{ EeV}$. These numbers can also very roughly be estimated from Fig. 4. Anisotropies of this size should be easily detectable by a full sky observatory such as the Pierre Auger project [21] which is currently under construction.

We note in this context that we have assumed in all our simulations that the source emits only protons. If the source is sufficiently compact, protons could convert into neutrons within the source. As pointed out in Ref. [22], for sources as close as Cen-A, neutrons at the highest energies could survive decay and produce a spike in the direction of the source. This can only increase anisotropy. Preliminary simulations performed with our code indicate that the total flux in the $\simeq 2^\circ$ pixel centered on the source is significantly (i.e. by a factor $\simeq 2$) increased only above $\simeq 300 \text{ EeV}$.

We stress that $B \simeq 1 \mu\text{G}$ corresponds to the upper limit inferred on the strength of the magnetic field in the Local Supercluster from Faraday rotation observations of distant quasars [12–14]. Strictly speaking, the rotation measure is a function of $B\sqrt{L}$, where L denotes as before the coherence scale of the field, provided that $L \ll R$, where R represents the size of the medium pervaded by the magnetic field (for the Local Supercluster $R \simeq 10 - 50 \text{ Mpc}$). In principle, the coherence length L could be smaller than 1 Mpc , used in the previous Section, and B correspondingly larger. However, as will be discussed in the next Section, the diffusion coefficient $D(E)$ scales inversely proportional with L , so that by decreasing L , one would increase $D(E)$ correspondingly, and the diffusion approximation would break down at a smaller energy, thereby increasing the anisotropy at higher energies. We thus find that one cannot decrease L and increase B to improve the fit to the data. Moreover, notwithstanding this fact, if diffusion were to be more efficient at the highest energies observed, the effective distance traveled would be consequently increased, and the GZK cut-off would be more pronounced, which would further aggravate the disagreement with the observed spectrum.

We thus conclude that $B \simeq 1 \mu\text{G}$ seems to be the only value of B that would be marginally consistent with Cen-A as the source of observed UHECRs. We further note that if equipartition of energy holds, the magnetic field intensity is tied to the thermal energy density of the am-

bient gas:

$$B = 0.5 \mu\text{G} T_7^{1/2} \kappa_{10}^{1/2} h_{70}, \quad (2)$$

where $T_7 \equiv T/10^7 \text{ K}$ is the temperature of the Local Supercluster in units of 10^7 K , and $\kappa_{10} \equiv \kappa/10$, with κ the collapse factor (i.e., the local overdensity of baryons and electrons), and h_{70} the Hubble constant in units of 70 km/s/Mpc . The gas cools by bremsstrahlung emission in the keV range, which in principle can be observed. A marginal detection of X-ray emission correlated with the plane of the Local Supercluster has actually been reported and corresponds to a collapse factor $\kappa_{10} \simeq 1$, with a weak dependence on the assumed temperature $T \simeq 10^8 \text{ K}$ [23]; the signal is however weak and these parameters could be in error. Numerical simulations of large-scale structure formation indicate that $\kappa_{10} \simeq 1$ and $T \simeq 10^7 \text{ K}$ are probably upper limits for sheets such as the Local Supercluster, and seem to better describe the filamentary structures [13]. Deep searches for soft X-ray emission correlated with the plane of the Local Supercluster using the XMM-Newton or Chandra observatories could improve these limits, and appear mandatory.

III. COMPARISON WITH ANALYTICAL ESTIMATES

Let us now compare these results with analytical estimates in an approach similar to [19]. There is often confusion in the literature about different regimes of diffusion and corresponding expressions for the diffusion coefficient. It is dangerous to take analytical expressions too literally as there exists no analytical derivation of diffusion coefficients in the limit in which the turbulent component of the magnetic fields becomes comparable or stronger than a (putative) uniform component, the so-called strong turbulence regime. In this respect, one should note that the formula for the diffusion coefficient given in Ref. [15], now used without caution in the community, does not correspond to an analytical derivation. It is a phenomenological formula, that is furthermore shown to be in error in Ref. [24], where analytical approximations and accurate measurements of diffusion coefficients obtained through Monte-Carlo simulations are presented. Notably, this latter study shows that for Kolmogorov turbulence the diffusion coefficient can be approximated as:

$$\begin{aligned} D(E) &\simeq 0.02 E_{20} B_{-6}^{-1} \text{Mpc}^2/\text{Myr} & E_{20} < E_c, \\ &\simeq 0.02 E_{20}^2 B_{-6}^{-2} L^{-1} \text{Mpc}^2/\text{Myr} & E_{20} > E_c. \end{aligned} \quad (3)$$

In this expression, E_{20} is the UHECR energy in units of 100 EeV , B_{-6} is the magnetic field strength in units of μG , L is in units of Mpc and $E_c = 1.45 B_{-6} L$ (in units of 100 EeV) corresponds to the condition $r_L = L/2\pi$, where $r_L = 0.11 E_{20} B_{-6}^{-1} \text{Mpc}$ is the Larmor radius. Note the difference of the above result with the formula given in

Ref. [15], for which $D(E) \propto E^{1/3}$ for $E_{20} < E_c$, and $D(E) \propto E$ for $E_{20} > E_c$. The dependence of $D(E)$ for $E < E_c$ in Eq. (3) above agrees with the phenomenological Bohm diffusion coefficient $D_B \simeq r_L c$ within a factor two.

The diffusive regime as well as the transition to nearly rectilinear propagation can also be seen in the dependence of time delay τ (defined as the difference between the total propagation time and the straight flight distance d/c) on energy E shown in Fig. 6 for $B_{-6} = 1$ and Cen-A as the source: In the diffusive regime the average time delay $\tau(E) \simeq d^2/4D(E)$, where d is the source distance, whereas for $E_{20} \gtrsim 3$, in the regime of almost rectilinear propagation, $\tau(E) \simeq 1.7 \times 10^8 \text{ yr} E_{20}^{-2} d_{\text{CenA}}^2 L B_{-6}^2$ [11], where $d_{\text{CenA}} \equiv d/3.4 \text{ Mpc}$. The values obtained for $D(E) \simeq d^2/4\tau(E)$ from Fig. 6 in the diffusive regime are consistent with Eq. (3) within the width of the distribution.

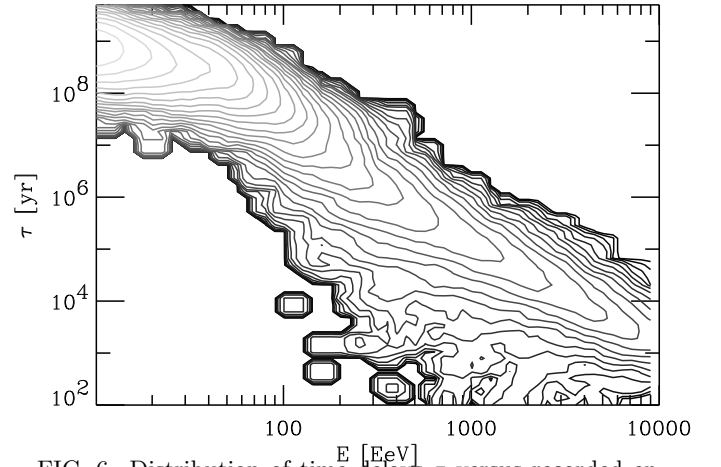


FIG. 6. Distribution of time delays τ versus recorded energy E , for $B = 1 \mu\text{G}$, and Cen-A as the source.

Note that according to Eq. (3) a largest eddy size L considerably smaller than 1 Mpc (which is not excluded) would lead to less diffusion, tending to make anisotropies even larger.

Using these results, one can understand the situation encountered in the previous section. In the diffusive regime one finds that the ratio of the diffusive propagation time (which is equal to the time delay in this approximation) to the source distance reads: $\tau(E)/d \simeq 16 E_{20}^{-2} B_{-6}^2 L d_{\text{CenA}}$, for $E_{20} > E_c$. Diffusion ceases to be a good approximation when $\tau(E)/d$ is no longer $\gg 1$. For instance, $\tau(E)/d > 2$ requires $E_{20} < 3 B_{-6} L^{1/2}$. This corresponds to a maximal energy for diffusion of $\simeq 100 \text{ EeV}$ when $B \simeq 0.3 \mu\text{G}$, and $\simeq 300 \text{ EeV}$ when $B \simeq 1 \mu\text{G}$. These numbers are in agreement with the results of the previous section. Note that the ratio of the diffusive propagation time to the source distance also corresponds to the ratio of the source distance to the mean free path for scattering on the magnetic inhomogeneities $\simeq D/c$ within a factor four.

The difference between our results and Ref. [19] can be explained as a misuse of the diffusion coefficient given in Ref. [15] by the authors of Ref. [19], and to some extent, by the fact that that diffusion coefficient itself has the wrong scaling with E , B , and L . More precisely in Ref. [19] the authors use the diffusion coefficient $D(E) \simeq 0.05 \text{ Mpc}^2/\text{Myr} E_{20}^{1/3} B_{-6}^{-1/3} L^{2/3}$ [15] (note that the present prefactor is the correct one; their Eq. (1) has a numerical error) on the whole energy range, whereas according to Ref. [15], this scaling is only valid when $r_L \lesssim L/2\pi$, or as above $E_{20} \lesssim E_c = 1.45 B_{-6} L$. This makes an important difference, because, had the authors of Ref. [19] used the other limiting regime they quote, namely $D \simeq 0.1 E_{20} B_{-6}^{-1} \text{ Mpc}^2/\text{Myr}$, valid for $E_{20} \gtrsim 1.45 B_{-6} L$, they would have found that the ratio of the diffusive distance traveled to source distance reads $d/4D \simeq 2.6 E_{20}^{-1} B_{-6} d_{\text{CenA}}$, which shows that $B > 1 \mu\text{G}$ is necessary to achieve diffusion up to the highest energies $E_{20} \simeq 3$. Instead, they used the former approximation, giving $d/4D \simeq 5.3 E_{20}^{-1/3} B_{-6}^{1/3} L^{-2/3} d_{\text{CenA}}$, which due to the (incorrect) weak scaling would let believe that diffusion can be achieved easily with $B \simeq 0.3 \mu\text{G}$ on the whole range of energies.

One should mention that the transition between diffusive and rectilinear regimes of propagation is not sudden; it stretches over half an order to an order of magnitude. As one approaches this transition, the anisotropy increases steeply to match the small angle deflection in the rectilinear regime $\theta_E \simeq 140^\circ E_{20}^{-1} B_{-6} L^{1/2} d_{\text{CenA}}^{1/2}$ [11]. Therefore it is incorrect to assume that the diffusive estimate for the anisotropy remains valid up to the transition energy.

Finally, Ref. [19] (unlike Ref. [22]) also base their calculations for the flux of particles detected at Earth on a time-dependent solution of the diffusion equation, but one should rather use a stationary solution corresponding to a continuously emitting source. Indeed if Cen-A were a bursting source, or more generally a source emitting only once on a timescale $t_{\text{em}} \ll \tau_{\text{min}}$, where τ_{min} is the smallest time delay imparted to all UHECRs, or equivalently, the time delay at the highest energies observed, an experiment like AGASA would record events only in a limited range of energies [25]. In other words the distance d_D of the diffusion front from the source at time t is given by $d_D(E) = 6D(E)t$, and depends on energy. At the present time at which AGASA is operating, the front of low energy particles would not have yet reached the Earth, while that of higher energy particles would already have passed. From Fig. 6 one sees that at any given time AGASA would record only part of the total energy spectrum, since particles with $E = 10 \text{ EeV}$ arrive at time $\tau \sim 10^9 \text{ yrs}$, while particles with $E = 100 \text{ EeV}$ arrive at times $\tau \sim 10^8 \text{ yrs}$.

This implies that if Cen-A is the source of all UHECRs, it has to be a continuously emitting source, or, what amounts to the same, an intermittent source that emits on timescales t_{em} , with quiescent periods of dura-

tion $\Delta t \ll \min[\Delta\tau(E)]$. Here $\Delta\tau(E)$ denotes the spread of time delays at energy E , and the condition ensures that the various contributions of the various bursts of particles largely overlap so as to produce a featureless energy spectrum at all times. Furthermore, since no low energy cut-off in the energy spectrum has been seen down to energies $\simeq 5 \text{ EeV}$, Cen-A must have been active for a time corresponding to the largest time delay possible $\simeq \tau(5 \text{ EeV}) + \Delta\tau(5 \text{ EeV})$. For $B \simeq 1 \mu\text{G}$, we find that Cen-A must have been producing UHECRs intermittently for the past $\simeq 10 \text{ Gyrs}$. Whether this is realistic or not can hardly be constrained on theoretical grounds. The above constraints on the duration of the periods of activity and quiescence t_{em} and Δt read $t_{\text{em}} \lesssim 10^7 \text{ yrs}$, and similarly for Δt , which are reasonable orders of magnitude for the evolution timescale of Cen-A [26]. The age of Centaurus A can be estimated from the time necessary for its jets to extend to their present size $\simeq 250 \text{ kpc}$, i.e. between $\sim 10^8 \text{ yrs}$ and a few Gyrs, depending on the deceleration during extension, so that for our purposes this age is essentially unknown. Note that Centaurus A is a radio-galaxy with sub-relativistic jets, and without hot spots; the lobes are not particularly active, with a total bolometric luminosity $\sim 10^{39} \text{ ergs/s}$ [26].

The constraints of Ref. [19] on the energy requirement must thus be reconsidered. In the stationary regime, the flux at Earth reads $E^2 j(E) = E^2 q(E)/(4\pi)^2 D(E)d$, where $q(E)$ is the injection spectrum at the source. One easily calculates that, assuming $q(E) \propto E^{-2}$, in order to produce the energy weighted flux measured by cosmic ray experiments $\simeq 10^{24.5} \text{ eV}^2 \text{ m}^{-2} \text{ s}^{-1} \text{ sr}^{-1}$, one requires a UHECR emission power $\mathcal{P}_{\text{UHECR}} \simeq 10^{39} B_{-6}^{-1} d_{\text{CenA}} \text{ ergs/s}$ at the source. Note that this represents the average power; the actual power during the phase of activity is higher and reads $\mathcal{P}_{\text{UHECR}}(t_{\text{em}} + \Delta T)/t_{\text{em}}$. The above $\mathcal{P}_{\text{UHECR}}$ is thus a strict lower limit, which is nevertheless more optimistic than the $\sim 10^{43} \text{ ergs/s}$ obtained in Ref [19].

As an aside, we note that the above constraint on the age of Centaurus A can be generalized to any such source of UHECRs, namely that the time delay at the lowest energies be smaller than the age of the source, and thus also the age of the Universe. The propagation time at 5 EeV reads, using Eq. (3): $\tau \simeq 2.8 \text{ Gyrs} B_{-6} d_{\text{CenA}}^2$. Imposing $\tau \leq 14 \text{ Gyrs}$ gives a general constraint between the distance d to the source and the strength of the intervening magnetic field:

$$\left(\frac{B}{1 \mu\text{G}}\right) \left(\frac{d}{10 \text{ Mpc}}\right)^2 \lesssim 0.6 \quad (4)$$

Even if there are several sources contributing to the cosmic ray flux, this limit should hold unless the sources conspire to add their individual piecewise contribution in such a way as to form a featureless energy spectrum. When there are many sources the above constraint disappears, as the central limit theorem would guarantee that a featureless spectrum would be produced; this is no-

tably one of the peculiarities of the γ -ray burst model of UHECR origin [27].

IV. CONCLUSIONS

Our detailed numerical simulations show that the model considered in Ref. [19], in which Centaurus A is the source of all observed UHECRs, is inconsistent with the data, at least for the magnetic field strength $B \simeq 0.3 \mu\text{G}$ put forward by these authors. We find that for a magnetic field strength $B \simeq 1 \mu\text{G}$, the predicted energy spectrum is in marginal agreement with that observed by AGASA. However the large deflection angle of the highest energy event (the Fly's Eye event) with respect to the line of sight to Cen-A must be explained as a $\simeq 2\sigma$ fluctuation. We also argued that this magnetic field intensity saturates the observational upper bounds from Faraday rotations and on X-ray emission from the ambient gas. This model can be tested by improving these upper limits with current experiments. We also showed that in order to explain all UHECRs down to $E \simeq 5 \text{ EeV}$, Cen-A must have been producing UHECRs for the past $\simeq 10 \text{ Gyrs}$. All these facts are rather strong requirements on the source and on the intervening magnetic fields. We thus find anew a conclusion obtained in previous studies [10,15–17], namely it is much more likely that a few sources within $\simeq 10 \text{ Mpc}$ from the Earth would produce the observed ultra-high energy cosmic ray flux, and that the ambient magnetic field strength in the Local Supercluster $B \simeq 0.1 - 0.5 \mu\text{G}$. Work is in progress to quantify the number of sources needed and the distance scale for various values of the magnetic field strength. Ongoing and future ultra-high energy cosmic ray experiments [5,6,21], by increasing the statistics at the highest energies, will soon provide much tighter bounds on the number of UHECR sources.

ACKNOWLEDGEMENTS

G.S. would like to thank Luis Anchordoqui, Pasquale Blasi, Glennys Farrar, Haim Goldberg, Tsvi Piran, and Tom Weiler for detailed discussions of this subject.

-
- [1] K. Greisen, Phys. Rev. Lett. 16 (1966) 748; G. T. Zatsepin and V. A. Kuzmin, Pis'ma Zh. Eksp. Teor. Fiz. 4 (1966) 114 [JETP. Lett. 4 (1966) 78].
 - [2] D. J. Bird et al., Phys. Rev. Lett. 71 (1993) 3401; Astrophys. J. 424 (1994) 491; ibid. 441 (1995) 144.
 - [3] See, e.g., M. A. Lawrence, R. J. O. Reid, and A. A. Watson, J. Phys. G 17 (1991) 733, and references therein; see also <http://ast.leeds.ac.uk/haverah/hav-home.html>
 - [4] N. N. Efimov et al., Proc. International Symposium on *Astrophysical Aspects of the Most Energetic Cosmic Rays*, eds. M. Nagano and F. Takahara (World Scientific Singapore, 1991) p.20; B. N. Afanasiev, Proc. of International Symposium on *Extremely High Energy Cosmic Rays: Astrophysics and Future Observatories*, ed. M. Nagano (Institute for Cosmic Ray Research, Tokyo, 1996), p.32.
 - [5] D. Kieda et al., Proc. of the 26th ICRC, Salt Lake, 1999; www.physics.utah.edu/Resrch.html
 - [6] Takeda et al., Astrophys. J. 522 (1999) 225; M. Takeda et al., Phys. Rev. Lett. 81 (1998) 1163; Hayashida et al., e-print astro-ph/0008102; www.akeno.icrr.u-tokyo.ac.jp/AGASA/.
 - [7] for recent reviews see J. W. Cronin, Rev. Mod. Phys. 71 (1999) S165; P. Bhattacharjee and G. Sigl, Phys. Rept. 327 (2000) 109; A. V. Olinto, Phys. Rept. 333-334 (2000) 329; X. Bertou, M. Boratav, and A. Letessier-Selvon, Int. J. Mod. Phys. A15 (2000) 2181;
 - [8] see, e.g., P. L. Biermann, J. Phys. G: Nucl. Part. Phys. 23, 1 (1997).
 - [9] G. Sigl, D. N. Schramm, and P. Bhattacharjee, Astropart. Phys. 2 (1994) 401
 - [10] J. W. Elbert, and P. Sommers, Astrophys. J. 441 (1995) 151;
 - [11] E. Waxman and J. Miralda-Escudé, Astrophys. J. 472 (1996) L89.
 - [12] J. P. Vallée, Fundamentals of Cosmic Physics, Vol. 19 (1997) 1.
 - [13] D. Ryu, H. Kang, and P. L. Biermann, Astron. Astrophys. 335 (1998) 19.
 - [14] P. Blasi, S. Burles, and A. V. Olinto, Astrophys. J. 514 (1999) L79.
 - [15] P. Blasi and A. V. Olinto, Phys. Rev. D. 59 (1999) 023001.
 - [16] G. Sigl, M. Lemoine, and P. Biermann, Astropart. Phys. 10 (1999) 141.
 - [17] M. Lemoine, G. Sigl, P. Biermann, e-print astro-ph/9903124.
 - [18] E.-J. Ahn, G. Medina-Tanco, P. L. Biermann, and T. Stanev, e-print astro-ph/9911123.
 - [19] G. R. Farrar and T. Piran, e-print astro-ph/0010370.
 - [20] G. Medina-Tanco and T. A. Ensslin, Astropart. Phys., to appear, e-print astro-ph/0011454.
 - [21] J. W. Cronin, Nucl. Phys. B (Proc. Suppl.) 28B (1992) 213; The Pierre Auger Observatory Design Report (2nd edition), March 1997; see also <http://www.auger.org/> and <http://www.lpnhep.in2p3.fr/auger/welcome.html>.
 - [22] L. A. Anchordoqui, H. Goldberg, and T. Weiler, e-print astro-ph/0103043.
 - [23] S.P. Boughn, ApJ 526, 14 (1999).
 - [24] F. Cassé, M. Lemoine and G. Pelletier, in preparation.
 - [25] J. Miralda-Escudé and E. Waxman, Astrophys. J. 462 (1996) L59.
 - [26] F. P. Israel, Astron. Astrophys. Rev. 8, 237 (1998).
 - [27] E. Waxman, Phys. Scripta T85, 117 (2000), and references therein.